



DIGITAL ACCESS TO SCHOLARSHIP AT HARVARD

Scara1 deficiency impairs clearance of soluble Amyloid- by mononuclear phagocytes and accelerates Alzheimer's-like disease progression

The Harvard community has made this article openly available. [Please share](#) how this access benefits you. Your story matters.

Citation	Frenkel, Dan, Kim Wilkinson, Lingzhi Zhao, Suzanne E. Hickman, Terry K. Means, Lindsey Puckett, Dorit Farfara, Nathan D. Kingery, Howard L. Weiner, and Joseph El Khoury. 2013. "Scara1 deficiency impairs clearance of soluble Amyloid- by mononuclear phagocytes and accelerates Alzheimer's-like disease progression." Nature communications 4 (1): 2030. doi:10.1038/ncomms3030. http://dx.doi.org/10.1038/ncomms3030 .
Published Version	doi:10.1038/ncomms3030
Accessed	April 17, 2018 4:42:35 PM EDT
Citable Link	http://nrs.harvard.edu/urn-3:HUL.InstRepos:11879346
Terms of Use	This article was downloaded from Harvard University's DASH repository, and is made available under the terms and conditions applicable to Other Posted Material, as set forth at http://nrs.harvard.edu/urn-3:HUL.InstRepos:dash.current.terms-of-use#LAA

(Article begins on next page)

Published in final edited form as:

Nat Commun. 2013 June 25; 4: 2030. doi:10.1038/ncomms3030.

Scara1 deficiency impairs clearance of soluble Amyloid- β by mononuclear phagocytes and accelerates Alzheimer's-like disease progression

Dan Frenkel^{1,¶,*}, Kim Wilkinson^{2,¶}, Lingzhi Zhao², Suzanne E. Hickman², Terry K. Means², Lindsey Puckett², Dorit Farfara¹, Nathan D. Kingery¹, Howard L. Weiner³, and Joseph El Khoury^{2,4,*}

¹Department of Neurobiology, George S. Wise Faculty of Life Sciences, Tel Aviv University, Tel Aviv, Israel

²Center for Immunology and Inflammatory Diseases, Massachusetts General Hospital, Harvard Medical School, CNY 149, Room 8301, 149 13th Street, Charlestown, Massachusetts 02129, USA

³Center for Neurologic Diseases, Brigham and Women's Hospital, Harvard Medical School, Boston, MA 02115, USA

⁴Division of Infectious Diseases, Massachusetts General Hospital, Harvard Medical School, CNY 149, Room 8301, 149 13th Street, Charlestown, Massachusetts 02129, USA

Abstract

In Alzheimer's disease soluble amyloid beta (sA β) causes synaptic dysfunction and neuronal loss. Receptors involved in clearance of sA β are not known. Here we use shRNA screening and identify the scavenger receptor *Scara1* as a receptor for sA β expressed on myeloid cells. To determine the role of *Scara1* in clearance of sA β *in vivo*, we cross *Scara1* null mice with PS1-APP mice, a mouse model of Alzheimer's disease and generate PS1-APP- *Scara1*-deficient mice. *Scara1* deficiency markedly accelerates A β accumulation leading to increased mortality. In contrast, pharmacological upregulation of *Scara1* expression on mononuclear phagocytes increases A β clearance. This approach is a potential treatment strategy for Alzheimer's disease.

Keywords

Microglia; monocytes; Alzheimer's disease; Transgenic mice; Amyloid; Phagocytosis; Degradation; Protollin; Scavenger receptor

Introduction

Work in transgenic mouse models of Alzheimer's disease (AD) indicates that mononuclear phagocytes can promote the clearance of amyloid- β (A β) peptides. Reduction in the number

*Correspondence should be addressed to JEK (jelkhoury@partners.org) or DF (dfrenkel@tauex.tau.ac.il).

¶Contributed equally to the work.

Author Contributions

DF and KW designed, performed and analyzed experiments. LZ, SH, TK, LP, DF, NK, performed and analyzed experiments, HLW designed experiments and edited manuscript, JEK designed, supervised and analyzed experiments, and wrote the manuscript.

Competing Financial Interests

The authors have no competing financial interests.

of recruited mononuclear phagocyte led to accelerated A β deposition especially around blood vessels, leading to intracerebral hemorrhage and increased mortality in a mouse model of AD¹. In support of these findings, depletion of perivascular macrophages significantly increased the number of Thioflavin S-positive cortical blood vessels and total perivascular A β levels². Conversely, stimulation of perivascular macrophage turnover or enhancing recruitment of peripheral monocytes reduced cerebral perivascular and parenchymal A β load^{2,3}. These data suggest that mononuclear phagocytes may delay progression of AD by promoting clearance of A β and preventing senile plaque formation. However, persistent A β accumulation in spite of increasing mononuclear phagocyte numbers in AD suggests that the ability of these cells to clear A β may decrease with age and progression of AD pathology⁴.

Much attention has been focused for many years on the insoluble aggregates of A β found in senile plaques. Insoluble fibrillar aggregates are neurotoxic *in vitro* and activate microglia and astrocytes to produce cytokines, chemokines and reactive oxygen and nitrogen species⁵, however, the number of senile plaques in any particular areas of the brain does not always correlate with neuronal death or synaptic loss in that area⁶⁻⁸. Such discrepancy brought attention to other non-aggregated forms of A β ^{9,10}. These soluble forms of A β (sA β) include A β monomers or oligomers that remain soluble in aqueous buffers after high speed ultracentrifugation^{9,10}. sA β may start accumulating in the brain before formation of visible senile plaques. sA β is associated with cognitive dysfunction in transgenic mice and several groups confirmed that a strong correlation exists between sA β levels and synaptic loss and neuronal degeneration⁶⁻¹². It is not known whether sA β interacts with monocytes or microglia or the potential receptors involved in such interactions. However, since sA β starts accumulating before formation of senile plaques and microglia are constantly surveying their environment for any potential injurious stimuli¹³ we hypothesized that mononuclear phagocytes can recognize and bind sA β .

Microglia and macrophages express several receptors that can promote binding and/or phagocytosis of fibrillar A β aggregates *in vitro*. These include the class A1 scavenger receptors (*Scara1*)¹⁴, the class B2 scavenger receptors (*Scarb2*) or CD36^{5,15}, RAGE¹⁶ and others. Mononuclear phagocytes also express a number of A β degrading enzymes, such as insulysin, neprilysin and others^{4,17}. The exact role of each of these receptors in development or progression of AD is not known. We found that as transgenic AD mice age, expression of these A β phagocytic receptors and A β degrading enzymes decreased significantly in microglia, thereby promoting A β accumulation and contributing to neurodegeneration⁴. This led us to hypothesize that restoring the ability of mononuclear phagocytes to phagocytose or degrade A β may be a therapeutic modality to delay or stop the progression of AD. In support of this hypothesis, genetic downregulation of the TGF β -Smad2/3 innate immune signaling pathway, led to increased infiltration of macrophages around blood vessels, and decreased A β levels and behavioral deficits in AD mice³. It is not known if pharmacological stimulation of mononuclear phagocyte A β clearance pathways will also lead to mitigation of AD-like pathology.

In this paper we use a shRNA screen to identify receptors for sA β and show that *Scara1* is a phagocytic receptor that mediates clearance of sA β *in vitro*, and that *Scara1* deficiency is associated with increased early mortality and A β deposition in the PS1-APP mouse model of AD. We also show that pharmacological upregulation of *Scara1* leads to increased A β clearance suggesting that this approach may be a strategy for treatment of AD.

Results

ShRNA screen identifies *Scara1* as a receptor for sA β uptake

To identify mononuclear phagocyte receptors involved in the uptake of sA β we used a mouse shRNA library targeting innate immune receptors to screen for genes that mediate macrophage uptake of sA β labeled with the fluorescent dye Hilyte-Fluor 488. We confirmed that our Hilyte-Fluor 488 A β is soluble using native electrophoresis and Thioflavin S staining (Supplementary Fig. S1a,b) as described⁵⁻⁸. The RNAi Consortium has previously published that its lentiviral library silences genes in a diverse set of cell types, contains 5 shRNA for nearly every gene in the murine genome, and is capable of significantly reducing target mRNA levels (Fig. 1a)¹⁸. Using a subset of the mouse lentiviral shRNA library targeting toll-like receptors, scavenger receptors and other pattern recognition receptors¹⁹, we performed a screen to identify genes that mediate macrophage uptake of sA β 1-42-Hilyte Fluor 488 using RAW 264.7 (RAW) macrophages. Silencing expression of all receptors tested was effectively performed to ~20% of normal expression (Fig. 1a and not shown). Interestingly, only silencing of the scavenger receptors CD36 and *Scara1*, led to a significant reduction in sA β 1-42-Hilyte Fluor 488 uptake by RAW macrophages (Fig. 1b and data not shown). The results of our shRNA screen indicate that *Scara1* and CD36 can mediate uptake of sA β by mononuclear phagocytes *in vitro*. Gene silencing of other scavenger receptors such as *Scarb1*, *Scarf*, *CD68*, and *CXCL16* also expressed by macrophages, had no effect on uptake of sA β 1-42-Hilyte Fluor 488 by RAW cells (Fig. 1b), suggesting that *Scara1* and CD36 are the main receptors involved in this process.

To confirm that uptake of sA β by microglia is indeed a receptor-mediated event, we incubated N9 microglia with increasing concentrations of sA β and quantified uptake by flow cytometry. As seen in fig.2a, uptake of sA β by microglia began to reach saturation at ~2 μ M. In addition, uptake of sA β by N9 microglia was time dependent and reached saturation at ~4 hours (Fig. 2b). These data indicate that uptake of sA β by microglia is likely to be receptor-mediated and is saturable in a dose and time-dependent manner. To further confirm that uptake of sA β by microglia is mediated by scavenger receptors, we incubated N9 cells for two hours with 1 μ M sA β 1-42-Hilyte Fluor 488 \pm 200 μ M Fucoidan, a broad inhibitor of scavenger receptors, and measured uptake by flow cytometry. Fucoidan significantly inhibited the amount of sA β taken by N9 microglia (Fig. 2c) and the number of cells that took sA β (Fig. 2d).

Scara1 deficiency is associated with reduced sA β uptake

Expression of *Scara1* in HEK293 cells is sufficient to promote the ability of these cells to take A β (Supplementary Fig. S2). To determine if *Scara1* is necessary for uptake of sA β by primary monocytes and microglia as suggested by our shRNA screen in macrophages, we isolated circulating monocytes and microglia from adult mice with targeted deletion of various scavenger receptors and from WT mice and tested the ability of these freshly isolated monocytes and microglia to take up sA β . Interestingly, only targeted deletion of *Scara1*, led to a significant reduction in the uptake of sA β by fresh monocytes (Fig. 3a) and microglia (Fig. 3b) by 65% and 50% respectively. Targeted deletion of CD36 did not affect uptake of sA β by monocytes and only reduced its binding to microglia by 25%, which was not statistically significant. These data indicate that *Scara1* is a major receptor for uptake of sA β by monocytes and microglia and that *Scara1*-mediated uptake is not redundant. The lack of effect of targeted deletion of CD36 on sA β uptake suggests that unlike *Scara1*, CD36 does not play a non-redundant role in clearance of sA β . Since targeted deletion of CD36 leads to reduced A β -induced activation of mononuclear phagocytes to produce cytokines and reactive oxygen species, our data suggest that CD36 may be involved in the activation of mononuclear phagocytes by sA β and not in the clearance of sA β by these cells^{5, 20, 21}.

This is reminiscent of the role CD36 plays in the interaction between macrophages and oxidized low density lipoproteins²².

Increased mortality in PS1-APP-Scara1^{-/-} mice

To determine if *Scara1* mediates clearance of sA β *in vivo*, and the effects of such clearance on accumulation of A β we generated PS1-APP-*Scara1*^{-/-} mice and analyzed these mice for A β levels and AD-like pathology. To accomplish this we utilized a strategy that we have successfully used in the past to generate transgenic APP mice deficient in the chemokine receptor *Ccr2*¹. Briefly, PS1-APP mice on a C57BL6 background were crossed to *Scara1*^{-/+} mice (also on a C57BL6 background) to generate PS1-APP-*Scara1*^{+/-} mice. We then crossed these mice to *Scara1*^{-/-} mice to generate PS1-APP-*Scara1*^{-/-} mice. PS1-APP-*Scara1*^{+/-} and PS1-APP-*Scara1*^{-/-} mice initially appeared healthy, without obvious behavioral abnormalities. However, after reaching 7 weeks of age, there was a marked increase in the mortality rate of both PS1-APP-*Scara1*^{+/-} and PS1-APP-*Scara1*^{-/-} mice as compared to control PS1-APP mice (Fig. 4a). By 160 d of age, 39% of PS1-APP-*Scara1*^{+/-} and 53% of PS1-APP-*Scara1*^{-/-} mice had died, compared to 16% of PS1-APP mice. The number of dying PS1-APP-*Scara1*^{+/-} mice reached a plateau at age 108 d, in contrast PS1-APP-*Scara1*^{-/-} mice continued to die until our data collection had stopped by age 160d. And while PS1-APP-*Scara1*^{-/-} mice had higher mortality at 160 days than PS1-APP-*Scara1*^{+/-} mice the overall difference between those two genotypes did not reach statistical significance (Fig. 4a). These data show that *Scara1* deficiency leads to increased mortality in mice expressing the PS1-APP transgenes. These data are similar to what we found with *Ccr2* deficiency (a defect that leads to reduced mononuclear phagocyte recruitment but does not affect their function¹). These data indicate that blocking mononuclear phagocyte number or function has detrimental effect in AD mouse models.

As expected, *Scara1* mRNA levels in the brains of PS1-APP-*Scara1*^{+/-} mice were ~45% of those in PS1-APP mice and were not detectable in PS1-APP-*Scara1*^{-/-} mice as determined by quantitative real-time PCR (qPCR) (Fig. 4b). A similar trend was observed in WT, *Scara1*^{+/+} and *Scara1*^{-/-} mice (not shown). Interestingly, analysis of *Scara1* protein expression by Western blot showed that 55% reduction in *Scara1* gene dosage (as occurs in *Scara1*^{+/-} mice) is associated with a much larger 76% reduction in *Scara1* protein level (Fig. 4 c and d). Since survival of PS1-APP mice appears to correlate with *Scara1* expression, it is possible that efficient clearance of A β requires a certain threshold of *Scara1* expression, the disproportionate reduction in *Scara1* protein levels in *Scara1*^{+/-} mice-likely below such threshold-may explain the comparable mortality rates between PS1-APP-*Scara1*^{+/-} and PS1-APP-*Scara1*^{-/-} mice.

Increased A β accumulation in PS1-APP-Scara1^{-/-} mice

To determine the effect(s) of *Scara1* deficiency on AD like pathology, we analyzed the brains of 8 months old PS1-APP-*Scara1*^{-/-} mice for A β deposition in comparison to PS1-APP mice. As seen in Fig.4e-g, *Scara1* deficiency led to a significant increase in the surface area fraction of the brain stained for A β in PS1-APP mice. As expected WT mice did not have any A β in their brain at this age (Fig. 2e). These data support the results obtained from our shRNA screen and from the experiments showing decreased uptake of sA β *in vitro* by monocytes and microglia isolated from *Scara1*^{-/-} mice (Fig.3a-b). The data further indicate that *Scara1* is a major receptor involved in endogenous clearance of A β and that deficiency in *Scara1*, as occurs in aging AD mice⁴, is associated with increased A β levels.

Our shRNA screening data showed that CD36 can mediate uptake of sA β . RAGE has been also shown to be a receptor for A β ¹⁶. To determine if *Scara1* deficiency indirectly affected CD36 or RAGE expression, we measured CD36 and RAGE mRNA in young (150 days)

WT, *Scara1*^{-/-}, PS1-APP and PS1-APP-*Scara1*^{-/-} brains by qPCR. As seen in Figure 5a, *Scara1* deficiency did not affect CD36 mRNA levels in *Scara1*^{-/-} or PS1-APP-*Scara1*^{-/-} brains. Furthermore, we did not detect any difference in expression of RAGE, in PS1-APP-*Scara1*^{-/-} mice compared to PS1-APP mice (Not shown). These data indicate that increased A β deposition in PS1-APP-*Scara1*^{-/-} brains are likely due to decreased *Scara1*-mediated A β clearance in these mice and not due to a change in expression of other A β receptors such as Cd36 and RAGE.

A β levels are also regulated by several A β -degrading enzymes such as neprilysin and insulin¹⁷. To determine if increased A β levels in the brains of PS1-APP-*Scara1*^{-/-} mice are associated with reduced expression of neprilysin and/or insulin, we measured mRNA levels of these two enzymes in the brains of young (150 days) WT, *Scara1*^{-/-}, PS1-APP and PS1-APP-*Scara1*^{-/-} mice. We found that expression of insulin and neprilysin was comparable in WT and *Scara1*^{-/-} mice. Interestingly, expression of neprilysin was significantly higher in young PS1-APP mice compared to WT mice suggesting that early in the disease process, uptake of A β may be associated with increased A β degradation. Expression of insulin was also slightly higher in PS1-APP mice compared to WT mice, but the difference was small and did not reach statistical significance (Fig. 5b, c). In contrast, both neprilysin and insulin expression was significantly reduced by 38% and 36% respectively in PS1-APP-*Scara1*^{-/-} brains as compared to PS1-APP brains (Fig. 5b,c). These data suggest that phagocytosis of A β in young PS1-APP mice is associated with increased A β degradation, whereas decreased uptake of A β , as occurs in PS1-APP-*Scara1*^{-/-} mice, leads to decreased A β degradation and further increase in A β accumulation thereby initiating a self-propagating loop of events that lead to accelerated disease progression.

Data shown in figure 4a indicate that mortality of PS1-APP-*Scara1*^{+/-} mice was only slightly better than that of PS1-APP-*Scara1*^{-/-} but the difference did not reach statistical significance. To determine if partial *Scara1* deficiency also affected AD-like pathology, we analyzed the brains of young (150 days) PS1-APP-*Scara1*^{+/-} mice for A β deposition in comparison to PS1-APP mice. As seen in supplementary figure S3a, PS1-APP-*Scara1*^{+/-} mice exhibited a significant increase in A β levels as measured by ELISA (700 pg/mg brain protein vs. 1500 pg/mg protein p<0.002). This increase also correlated with increased visible A β deposits (Supplementary Fig. S3b and c).

Of note, the number of visible A β deposits in ~150 days old PS1-APP and PS1-APP-*Scara1*^{+/-} mice were small (Supplementary Fig. S3b and c), and we did not detect any Thioflavin S+ deposits (not shown) suggesting that the majority of A β measured in these mice is in soluble or non-aggregated form. These data support the results obtained from our shRNA screen and from the experiments showing decreased uptake of sA β *in vitro* by monocytes and microglia isolated from *Scara1* deficient mice.

Upregulation of *Scara1* leads to increased A β clearance

Protollin, a proteosome-based adjuvant comprised of purified outer membrane proteins of *Neisseria meningitidis* and lipopolysaccharide that is well tolerated in humans²³, promotes increased accumulation of mononuclear phagocytes and increased clearance of amyloid when given intranasally to transgenic AD mice^{24, 25}. We investigated whether the mechanism by which Protollin enhances A β uptake by mononuclear phagocytes involves upregulation of *Scara1* or CD36. As seen in figure 6a–c, while Protollin upregulated mRNA levels of *Scara1* by more than 3 fold, it didn't affect mRNA levels of CD36. Furthermore, Protollin upregulated *Ccl2* mRNA levels by ~7fold (Fig. 6d). These data suggest that the increased numbers of mononuclear phagocytes observed in Protollin treated Alzheimer's mice, may be due to their recruitment to sites of A β deposition via *Ccl2*. These data also

suggest that Protollin-induced enhanced A β clearance, may in part be due to increased recruitment of mononuclear phagocytes to A β deposition sites.

Clearance of A β deposits *in situ* from brain sections derived from transgenic AD mice has been used as a surrogate measure for astrocyte ability to clear A β *in vivo*²⁶. To test if Protollin-induced activation of N9 microglia, promotes the ability of these cells to reduce A β deposits, we incubated these cells with brain sections derived from aged transgenic PS1-APP brains in the presence of increasing concentrations of Protollin. Such sections normally exhibit florid A β deposits in the cortex and hippocampus. As seen in figures 6e and 6f, the addition of Protollin-stimulated N9 microglia, significantly reduced the size and number of A β deposits in such sections in the hippocampus when compared to untreated sections, or to sections incubated with unstimulated N9 microglia. To determine the relative importance of *Scara1* in A β clearance by microglia activated with Protollin, we isolated WT and *Scara1*^{-/-} adult microglia as previously described²⁶ and compared their ability to clear brain A β deposits from PS1-APP brain slices as we did with N9 cells. After incubation of the brain sections with microglia from WT mice for 72 h, there was a 58% reduction in total A β deposits in the hippocampus (p=0.0013) as compared to untreated sections and to sections incubated with microglia from *Scara1*^{-/-} mice (p=0.0214), which showed only a 20% reduction (p=0.0317) as compared to untreated section (Fig. 6g,h). These data strongly support that Protollin-induced increased A β clearance is in part dependent on *Scara1* and that pharmacologic upregulation of *Scara1* expression can be successfully accomplished.

Discussion

The role of mononuclear phagocytes including peripheral monocytes and microglia in Alzheimer's disease is subject to intense investigation²⁷. While a shotgun approach that deletes all microglia for a brief period of time did not show an effect on amyloid deposition in a transgenic AD mouse model²⁸, targeted genetic manipulation of the innate immune system in mouse models of Alzheimer's disease provided strong evidence that mononuclear phagocytes play critical roles in regulating A β deposition by regulating A β clearance pathways. Indeed, defects in microglial/mononuclear phagocytes accumulation in transgenic APP mice and other mouse models of AD are associated with increased A β deposition and increased mortality and/or cellular toxicity in these mice^{1, 29}. Furthermore, deficiencies and/or mutations in specific innate immune receptors such as CD14 and TLR4 affect A β deposition^{30, 31}. Unfortunately, with aging and progression of Alzheimer's disease, innate immune cells of the brain appear to become dysfunctional and their ability to clear amyloid becomes significantly reduced⁴. The exact mechanism(s) of such microglial dysfunction are not clear, but are believed to be due at least in part to downregulation of microglial A β phagocytic receptors⁴. In this manuscript, we provide direct evidence that the microglial/monocyte scavenger receptor *Scara1* is a key A β clearance receptor expressed by these cells and that genetic deficiency in *Scara1* is indeed associated with increased accumulation of A β . In addition, deficiency in *Scara1* is associated with increased mortality in PS1-APP mice. Such increases in mortality and A β deposition are similar to what we observed with APP-Ccr2-deficient mice and suggest that abnormalities in the number and/or function of mononuclear phagocytes can have detrimental effects on transgenic mouse models of AD. In contrast to the detrimental effects associated with dysfunction of the innate immune system in AD, we also show that restoring some of the A β -clearing ability of the innate immune system by pharmacological upregulation of *Scara1* leads to increased A β clearance by mononuclear phagocytes and microglia and therefore may be beneficial in slowing down or delaying progression of this disease. It is not clear if upregulating *Scara1* expression by non-pharmacological approaches will also lead to increased sA β clearance. Indeed, upregulating *Scara1* mRNA in aging AD mice following irradiation does not seem to have the same effect as using Protollin³². It is possible that such apparent discrepancy may be due to increased

influx of A β across the blood brain barrier (BBB) as a result of increased permeability of the BBB following irradiation, to differences in the age and genotype of the mice analyzed and/or the approach used to quantify sA β . Nonetheless, our data clearly indicate that upregulating *Scara1* expression pharmacologically, is a viable therapeutic strategy to treat AD.

We showed previously that blocking CD36-A β interactions reduces A β -induced activation of microglia to produce cytokines and reactive oxygen species^{5, 20}. We also showed that blocking these interactions does not affect phagocytosis of A β . Therefore data from these papers indirectly support our findings in this manuscript that *Scara1* rather than CD36 is the main receptor for clearance of A β by mononuclear phagocytes. Our data also suggest that *Scara1* and CD36 play complementary non-redundant roles in the interactions of mononuclear phagocytes with A β . *Scara1*-A β interactions are beneficial and promote phagocytosis and clearance of A β , whereas, CD36-A β interactions are harmful and lead to production of neurotoxins and pro-inflammatory molecules. This is reminiscent of the role CD36 plays in the interaction between macrophages and oxidized low density lipoproteins in atherosclerosis. Indeed we have shown in the past that while *Scara1* mediates adhesion to Oxidized LDL coated surfaces, CD36 mediates macrophage activation by Oxidized LDL to produce reactive oxygen species²². In this regard the findings presented in this manuscript draw an exciting not yet described parallel between atherosclerosis and AD. Dissecting the complex roles of various scavenger receptors in mononuclear phagocyte-A β interactions is therefore very important and as we are showing in this manuscript has therapeutic implications for AD.

Materials and Methods

shRNA lentiviral infections

Plasmids encoding lentiviruses expressing shRNAs were obtained from the RNAi Consortium (TRC) library TRC-Mm1.0¹⁸, purified using the QiaPrep miniprep kit (Qiagen) then transfected into HEK 293T cells with a three-plasmid system to produce lentivirus. Infection conditions were optimized in 96-well plates. 20,000 macrophages were placed in each well of 96-well tissue culture dishes and infected using 5 μ l of shRNA lentiviral supernatant and 7.5 μ g/ml polybrene. The cells were spun for 30 minutes at 2000 rpm and incubated for 24 hours. To select for shRNA integration, infected cells were placed in puromycin (3 μ g/ml) and RPMI containing 10% FBS. The cells were tested 1–2 weeks after infection.

Mice—PS1-APP mice bi-transgenic mice (B6C3-Tg (APP^{swe}, PSEN1^{dE9})85Dbo/J stock number 004462)^{33, 34} were purchased from The Jackson Laboratories (Bar Harbor, ME) and bred in the animal care facilities at Massachusetts General Hospital. Control mice are non-transgenic littermates of those PS1-APP mice expressing these transgenes.

Scara1^{-/-} mice were generated by professor Tatsuhiko Kodama, and a colony has been maintained in our lab for many years³⁵. CD36^{-/-} mice were generated by Dr. Kathryn Moore on a C57BL6 background and a colony has been maintained in our lab for many years⁵. PS1-APP, *Scara1*^{-/-} and CD36^{-/-} mice were backcrossed >13 generations on a C57BL/6 background. *Lox-1*^{-/-} mice³⁶ were a generous gift from professor Tatsuya Sawamura, National Cardiovascular Center Research Institute Osaka, JAPAN. *RAGE*^{-/-} mice³⁷ were a generous gift from professor Hiroshi Yamamoto, Kanazawa, Japan.

All protocols were approved by the Massachusetts General Hospital and Brigham and Women's Hospital Institutional Animal Care and Use Committees and met US National Institutes of Health guidelines for the humane care of animals.

Stimulation and cell surface staining of N9 microglia

N9 mouse microglia (a gift from Dr. P. Riciarrdi-Castagnoli, University of Milano, Bicocca, Italy)³⁸ were plated on 24-well plates coated with 1 μ g Fibronectin/cm² (Sigma-Aldrich), and grown overnight in RPMI supplemented with 10% FBS, L-glutamine (2mM), penicillin 10 IU/ml and streptomycin 10 μ g/ml. The following day, Protollin (Glaxo Smith Kline, Laval, Quebec, Canada) was added and cells were incubated overnight. For staining, cells were lifted from the plate with CellStripper™ (Mediatech), and resuspended in PBS/1% BSA/2% FBS containing 10 μ g/ml Fc block (AbD Serotec) then APC-labeled anti-mouse CD11b (1 μ g/ml) (BD Biosciences Pharmingen, San Diego, CA) or APC-labeled hamster anti-mouse CD36 clone HM36 (1 μ g/ml) (BioLegend, San Diego, CA) or Alexa647-labeled anti-CD204 (Scara1) clone 2F8 (2.5 μ g/ml) (AbD Serotec) or isotype-matched control antibodies (same concentrations as primary antibodies), were added and incubated on ice for 1 hour. Cells were then fixed and fluorescence intensity was measured using a FACScalibur™ (BD Biosciences, San Jose, CA) flow cytometer.

Isolation of CD11b⁺ microglia from adult brains

Adult mouse microglia were isolated as described⁴. Briefly, 12 week old mice were euthanized and perfused with 30cc PBS without Ca⁺⁺ and Mg⁺⁺ (PBS⁻). Brains were then rinsed, minced, and treated with Dispase and Collagenase Type 3 (Worthington Biochemicals, Lakewood, NJ), for 45 minutes at 37°C; followed by addition of 40U/ml DNase I grade II (Roche Applied Science, Indianapolis, IN) and incubation for an additional 15 minutes. The enzymes were inactivated by addition of 20ml Hanks Balanced Salt Solution without Ca⁺⁺ and Mg⁺⁺ (HBSS⁻) (Mediatech) containing 2mM EDTA and 2% fetal bovine serum (FBS) and the digested brain bits were triturated sequentially with a 25-, 10-, and 5-ml pipette (8–10 times each step) and passed over a 100 μ m filter (Fisher Scientific, Pittsburgh, PA). Cells were centrifuged and resuspended in RPMI /L glutamine and mixed with physiologic Percoll® (Sigma Aldrich), and centrifuged at 850 \times g for 45 minutes. The cell pellet was resuspended in RPMI and the cells were passed over a 70 μ m filter (Fisher Scientific), washed then passed over a 40 μ m filter (Fisher Scientific). The cells were then incubated with anti-mouse Cd11b-coated microbeads (Miltenyi Biotech, Auburn, CA) then washed. The bead-cell pellet was resuspended in PBS/0.5% BSA/2mM EDTA and passed over a magnetic MACS® Cell Separation column (Miltenyi Biotech) to separate Cd11b-positive cells (i.e. cells that bound the beads–microglia/mononuclear phagocytes) from unbound Cd11b-negative cells (CD11b^{neg}). Flow-through was collected and the column was rinsed 3 \times with PBS/BSA/EDTA. CD11b-positive cells (CD11b⁺) were eluted by removing the column from the magnetic holder and pushing PBS/BSA/EDTA through the column with a plunger. Cells were centrifuged and the pellets were resuspended in RPMI 1640 (Invitrogen) and used for experiments. Microglia isolated in this manner are more than 96% pure⁴.

Isolation of Monocytes from WT and KO mice

Monocytes were isolated by centrifugation over Ficoll 1077 as described for human monocytes^{39, 40}. This step removes neutrophils and red blood cells. The remaining cells include monocytes and Lymphocytes. This was followed by adhesion to tissue culture plates for 1 hour. The adherent cells (>90% monocytes) were then detached by brief incubation with 5 mM EDTA in PBS as described³⁹.

Quantitative Real Time PCR

Total RNA from each sample of cells (7.5–15 \times 10⁵ cells) was isolated using the RNeasy® Plus mini kit (Qiagen, Valencia, CA) according to the manufacturer's instructions and reverse transcribed using Multiscribe™ reverse transcriptase (Applied Biosystems, Foster

City, CA). Dilutions of each cDNA prep were used to assess β 2-microglobulin RNA levels and samples were then adjusted to give equivalent levels of β 2-microglobulin per well in subsequent qPCR reactions for other genes. The qPCR was performed with the MX4000™ unit (Agilent technologies, Santa Clara, CA) using SYBR Green to detect the amplification products as described^{1, 5}. The following cycles were performed: initial denaturation cycle 95°C for 10 min, followed by 40 amplification cycles of 95°C for 15 secs and 60°C for one min and ending with one cycle at 25°C for 15 secs. Relative quantification of mRNA expression was calculated by the comparative cycle method described by the manufacturer (Agilent technologies).

For *Scara1* qPCR, a standard curve for *Scara1* was prepared from a plasmid (Open Biosystems, Huntsville, AL) containing full-length mouse *Scara1* then whole brain RNA was isolated from triplicate samples using a Qiagen RNA easy Mini kit (Valencia, CA) and quantified using a Thermo-Fisher Nanodrop (Waltham, MA). 1 μ g RNA was reverse-transcribed into cDNA using Invitrogen's First Strand Synthesis kit (Carlsbad, CA), and qPCR performed in a Roche 480 Lightcycler qPCR machine (Indianapolis, IN) in triplicates for *Scara1* (Forward primer: TGAACGAGAGGATGCTGACTG, Reverse primer: GGAGGGGCCATTTTGTAGTGC) and compared to a standard curve of mouse *Scara1* cDNA

A β ELISA

For measurement of A β , we used commercially available ELISA kits (Invitrogen). Hemispheres of WT, PS1-APP and PS1-APP-*Scara1*^{+/-} mice were homogenized in buffer containing 0.02 M guanidine and ELISA for A β performed according to the manufacturer's instructions.

In vitro uptake of A β by N9 cells

N9 cells cultured in 6 well plates were incubated overnight with various concentrations of Protollin. The cells were then incubated with PBS containing 1% BSA and 500ng/ml A β 1–42 labeled with Alexa 488 (Anaspec, CA) for up to 4 hours, then washed 3 \times in PBS and lifted from the plate with CellStripper™ (Mediatech). Cells were then fixed by the addition of 2% PFA. Cell associated fluorescence intensity was measured using a FACScalibur™ (BD Biosciences, San Jose, CA) flow cytometer.

Uptake of A β from brain sections and Immunohistochemistry

Brains from transgenic PS1-APP were harvested and frozen unfixed in liquid nitrogen vapor and stored at -80°C and 10–14 μ m frozen sections were cut. N9 cells or WT microglia isolated from adult mice, were then added in the presence of Protollin and incubated at 37°C for 24 hours. Unbound cells were then rinsed in PBS and the sections fixed in 4% PFA. To stain for A β , sections were blocked in PBS / 0.3% Triton-X 100 / 2% goat serum for 30 minutes, then incubated overnight at 25°C with rabbit anti-pan A β antibody (Biosource, Camarillo, CA) or control antibody, at 2 μ g/ml in PBS containing 0.3% Triton X-100 and 2% goat serum. The slides were then processed using the Vectastain® Elite ABC Kit Rabbit IgG (Vector laboratories, Burlingame, CA) according to the manufacturer's instructions. Vector® NovaRed™ substrate kit for peroxidase (Vector Laboratories) was used to develop target-bound peroxidase for detection of A β in brain sections. Slides were counterstained with hematoxylin, mounted with VectaMount® (Vector Laboratories), visualized by brightfield microscopy and digitally photographed. Alternatively, secondary anti rabbit IgG antibodies labeled with Alexa488™ were used, the slides counterstained with DAPI and mounted using Vectashield® (Vector Laboratories) and digitally photographed. For quantitation of the percent surface area stained with Anti-A β , 5 equally spaced sections were used per brain.

Western blot of *Scara1*

2 μ g cell lysates were loaded onto a 10% SDS polyacrylamide gel (Invitrogen) transferred via iBlot® (Invitrogen) onto polyvinylidene difluoride (PVDF) membrane, blocked for 1 hour with 5% milk, then incubated with primary goat anti- mouse *Scara1* antibodies (R&D systems) followed by anti-goat horseradish peroxidase –labeled secondary antibody. The blots were then exposed to Hyperfilm™ (Amersham), developed and band intensity quantified by densitometry with image J software.

Statistical analysis

Statistical analysis was performed using one-way ANOVA with the Tukey test provided in the “Microcal Origin 8” graphics and statistics software. P values <0.05 were considered significant.

Supplementary Material

Refer to Web version on PubMed Central for supplementary material.

Acknowledgments

This work was supported by a grant from the HFSP and ISF and an NIRG grant from the Alzheimer’s Association to DF, by grant AG043975 to HLW and by NIH grants NS059005, AG032349, AI082660 and a grant from the Dana Foundation Neuroimmunology Program to JEK.

References

1. El Khoury J, et al. Ccr2 deficiency impairs microglial accumulation and accelerates progression of Alzheimer-like disease. *Nat Med.* 2007; 13:432–438. [PubMed: 17351623]
2. Hawkes CA, McLaurin J. Selective targeting of perivascular macrophages for clearance of beta-amyloid in cerebral amyloid angiopathy. *Proc Natl Acad Sci U S A.* 2009; 106:1261–1266. [PubMed: 19164591]
3. Town T, et al. Blocking TGF-beta-Smad2/3 innate immune signaling mitigates Alzheimer-like pathology. *Nat Med.* 2008; 14:681–687. [PubMed: 18516051]
4. Hickman SE, Allison EK, El Khoury J. Microglial dysfunction and defective beta-amyloid clearance pathways in aging Alzheimer's disease mice. *J Neurosci.* 2008; 28:8354–8360. [PubMed: 18701698]
5. El Khoury JB, et al. CD36 mediates the innate host response to beta-amyloid. *J Exp Med.* 2003; 197:1657–1666. [PubMed: 12796468]
6. Lue LF, et al. Soluble amyloid beta peptide concentration as a predictor of synaptic change in Alzheimer's disease. *Am J Pathol.* 1999; 155:853–862. [PubMed: 10487842]
7. McLean CA, et al. Soluble pool of Abeta amyloid as a determinant of severity of neurodegeneration in Alzheimer's disease. *Ann Neurol.* 1999; 46:860–866. [PubMed: 10589538]
8. Wang J, Dickson DW, Trojanowski JQ, Lee VM. The levels of soluble versus insoluble brain Abeta distinguish Alzheimer's disease from normal and pathologic aging. *Exp Neurol.* 1999; 158:328–337. [PubMed: 10415140]
9. Haass C, Selkoe DJ. Soluble protein oligomers in neurodegeneration: lessons from the Alzheimer's amyloid beta-peptide. *Nat Rev Mol Cell Biol.* 2007; 8:101–112. [PubMed: 17245412]
10. Sakono M, Zako T. Amyloid oligomers: formation and toxicity of Abeta oligomers. *Febs J.* 277:1348–1358. [PubMed: 20148964]
11. Lesne S, et al. A specific amyloid-beta protein assembly in the brain impairs memory. *Nature.* 2006; 440:352–357. [PubMed: 16541076]
12. Walsh DM, et al. Naturally secreted oligomers of amyloid beta protein potently inhibit hippocampal long-term potentiation in vivo. *Nature.* 2002; 416:535–539. [PubMed: 11932745]

13. Nimmerjahn A, Kirchhoff F, Helmchen F. Resting microglial cells are highly dynamic surveillants of brain parenchyma in vivo. *Science*. 2005; 308:1314–1318. [PubMed: 15831717]
14. El Khoury J, et al. Scavenger receptor-mediated adhesion of microglia to beta-amyloid fibrils. *Nature*. 1996; 382:716–719. [PubMed: 8751442]
15. Coraci IS, et al. CD36, a class B scavenger receptor, is expressed on microglia in Alzheimer's disease brains and can mediate production of reactive oxygen species in response to beta-amyloid fibrils. *Am J Pathol*. 2002; 160:101–112. [PubMed: 11786404]
16. Yan SD, et al. RAGE and amyloid-beta peptide neurotoxicity in Alzheimer's disease. *Nature*. 1996; 382:685–691. [PubMed: 8751438]
17. El Khoury Joseph, HSE. Mechanisms of Amyloid B clearance in Alzheimer's disease. Sun, M-K., editor. New York: Nova Biomedical Books; 2009.
18. Moffat J, et al. A lentiviral RNAi library for human and mouse genes applied to an arrayed viral high-content screen. *Cell*. 2006; 124:1283–1298. [PubMed: 16564017]
19. Means TK, et al. Evolutionarily conserved recognition and innate immunity to fungal pathogens by the scavenger receptors SCARF1 and CD36. *J Exp Med*. 2009; 206:637–653. [PubMed: 19237602]
20. Wilkinson K, Boyd JD, Glicksman M, Moore KJ, El Khoury J. A high-content drug screen identifies ursolic acid as an inhibitor of amyloid- β interactions with its receptor CD36. *J Biol Chem*.
21. Stewart CR, et al. CD36 ligands promote sterile inflammation through assembly of a Toll-like receptor 4 and 6 heterodimer. *Nat Immunol*. 11:155–161. [PubMed: 20037584]
22. Maxeiner H, et al. Complementary roles for scavenger receptor A and CD36 of human monocyte-derived macrophages in adhesion to surfaces coated with oxidized low-density lipoproteins and in secretion of H₂O₂. *J Exp Med*. 1998; 188:2257–2265. [PubMed: 9858512]
23. Fries LF, et al. Safety and immunogenicity of a proteosome-Shigella flexneri 2a lipopolysaccharide vaccine administered intranasally to healthy adults. *Infect Immun*. 2001; 69:4545–4553. [PubMed: 11401998]
24. Frenkel D, Maron R, Burt DS, Weiner HL. Nasal vaccination with a proteosome-based adjuvant and glatiramer acetate clears beta-amyloid in a mouse model of Alzheimer disease. *J Clin Invest*. 2005; 115:2423–2433. [PubMed: 16100572]
25. Frenkel D, et al. A nasal proteosome adjuvant activates microglia and prevents amyloid deposition. *Ann Neurol*. 2008; 63:591–601. [PubMed: 18360829]
26. Wyss-Coray T, et al. Adult mouse astrocytes degrade amyloid-beta in vitro and in situ. *Nat Med*. 2003; 9:453–457. [PubMed: 12612547]
27. El Khoury J. Neurodegeneration and the neuroimmune system. *Nat Med*. 16:1369–1370. [PubMed: 21135838]
28. Grathwohl SA, et al. Formation and maintenance of Alzheimer's disease beta-amyloid plaques in the absence of microglia. *Nat Neurosci*. 2009; 12:1361–1363. [PubMed: 19838177]
29. Bruban J, et al. CCR2/CCL2-mediated inflammation protects photoreceptor cells from amyloid-beta-induced apoptosis. *Neurobiol Dis*. 42:55–72. [PubMed: 21220018]
30. Reed-Geaghan EG, Reed QW, Cramer PE, Landreth GE. Deletion of CD14 attenuates Alzheimer's disease pathology by influencing the brain's inflammatory milieu. *J Neurosci*. 30:15369–15373. [PubMed: 21084593]
31. Song M, et al. TLR4 mutation reduces microglial activation, increases A β deposits and exacerbates cognitive deficits in a mouse model of Alzheimer's disease. *J Neuroinflammation*. 8:92. [PubMed: 21827663]
32. Mildner A, et al. Distinct and non-redundant roles of microglia and myeloid subsets in mouse models of Alzheimer's disease. *J Neurosci*. 31:11159–11171. [PubMed: 21813677]
33. Borchelt DR, et al. Accelerated amyloid deposition in the brains of transgenic mice coexpressing mutant presenilin 1 and amyloid precursor proteins. *Neuron*. 1997; 19:939–945. [PubMed: 9354339]
34. Jankowsky JL, et al. Co-expression of multiple transgenes in mouse CNS: a comparison of strategies. *Biomol Eng*. 2001; 17:157–165. [PubMed: 11337275]

35. Thomas CA, et al. Protection from lethal gram-positive infection by macrophage scavenger receptor-dependent phagocytosis. *J Exp Med.* 2000; 191:147–156. [PubMed: 10620613]
36. Mehta JL, et al. Deletion of LOX-1 reduces atherogenesis in LDLR knockout mice fed high cholesterol diet. *Circ Res.* 2007; 100:1634–1642. [PubMed: 17478727]
37. Yonekura H, Yamamoto Y, Sakurai S, Watanabe T, Yamamoto H. Roles of the receptor for advanced glycation endproducts in diabetes-induced vascular injury. *J Pharmacol Sci.* 2005; 97:305–311. [PubMed: 15750291]
38. El Khoury J, et al. Scavenger receptor-mediated adhesion of microglia to beta-amyloid fibrils. *Nature.* 1996; 382:716–719. [PubMed: 8751442]
39. el Khoury J, et al. Macrophages adhere to glucose-modified basement membrane collagen IV via their scavenger receptors. *J Biol Chem.* 1994; 269:10197–10200. [PubMed: 8144597]
40. Hickman SE, el Khoury J, Greenberg S, Schieren I, Silverstein SC. P2Z adenosine triphosphate receptor activity in cultured human monocyte-derived macrophages. *Blood.* 1994; 84:2452–2456. [PubMed: 7919365]

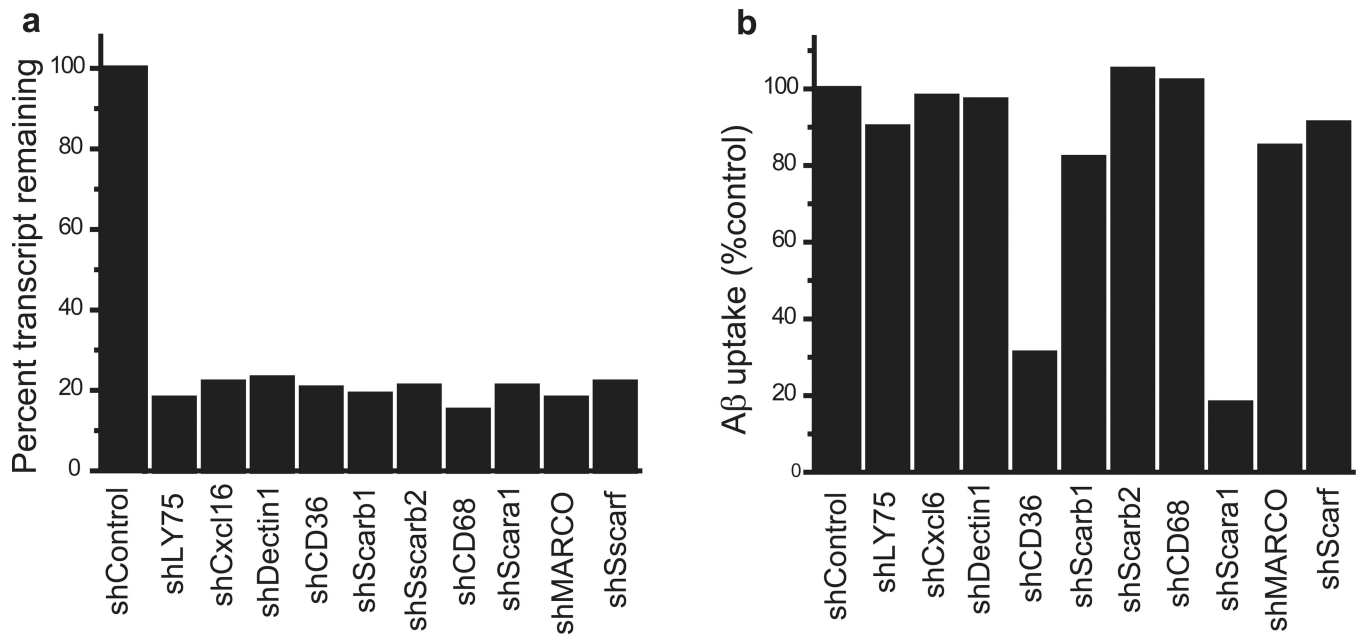


Figure 1. A shRNA screen identifies *Scara1* as a receptor for sA β

(a) RAW macrophages were transduced with lentivirus encoding gene-specific shRNAs to 30 pattern recognition receptors or with a control shRNA directed against GFP. Gene expression was measured by qPCR, and three to five individual shRNAs per gene were identified that significantly reduced mRNA expression. **(b)** Pattern recognition receptor expression was knocked down in individual pools of RAW macrophages, which were then incubated with Hilyte-fluor labeled sA β 1–42 for 2 h. Cell associated sA β was then quantified by flow cytometry. Data are from a representative experiments repeated 3 times with similar results.

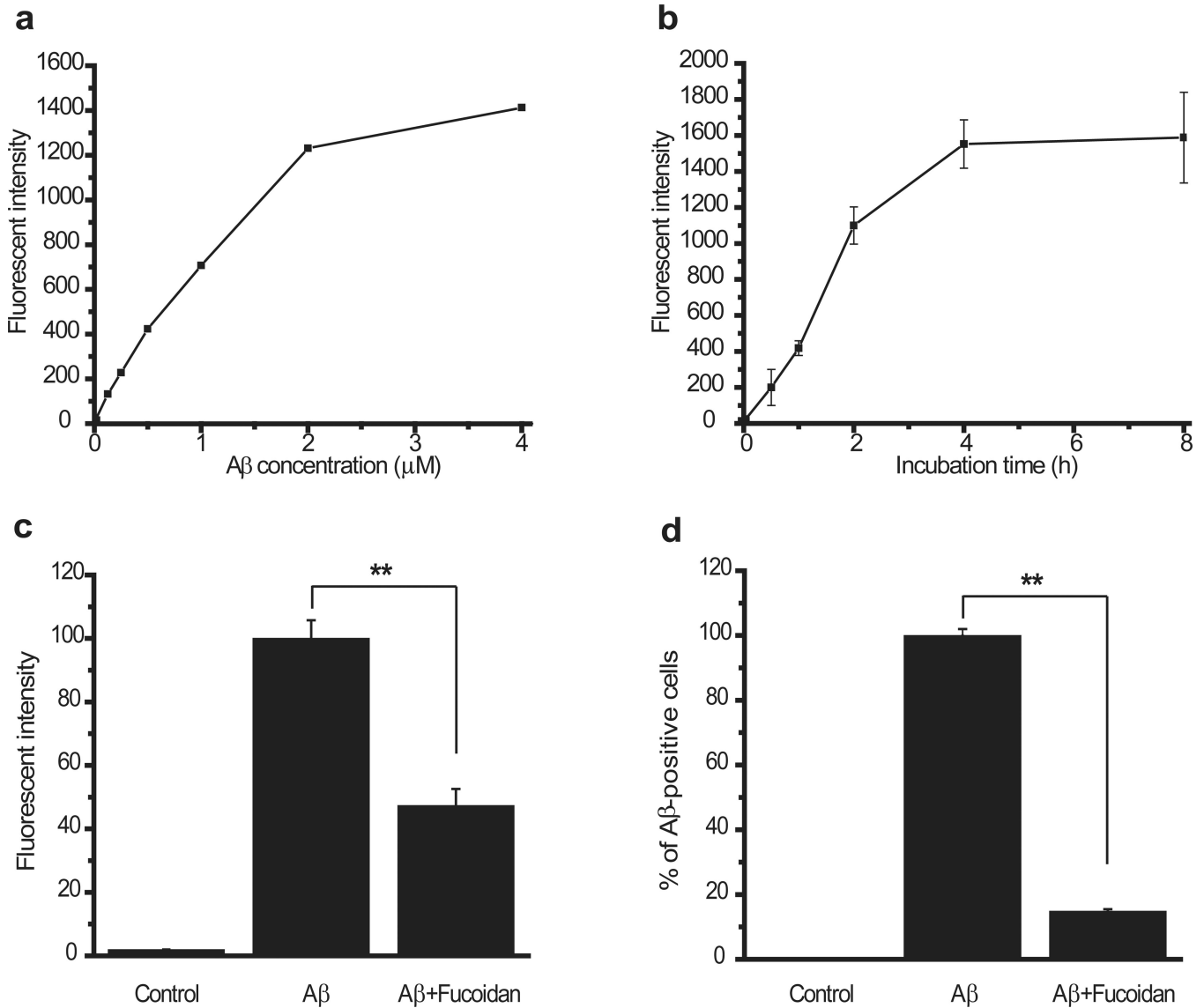


Figure 2. Uptake of sAβ by N9 microglia

(a, b) Uptake of Hilytefluor488-labeled sAβ by N9 microglia is saturable in a dose and time-dependent manner. (c, d) N9 cells were pretreated with 200μg/ml Fucoidan, a broad inhibitor of scavenger receptors, and then incubated with 1μM freshly dissolved Hilytefluor488-labeled sAβ 1–42 for 2 hours. The uptake of sAβ was measured by flow cytometry. Fucoidan significantly inhibited the amount of sAβ taken up by N9 cells and the number of cells that took sAβ indicating that microglial scavenger receptors are essential for phagocytosis of soluble Aβ. Values are mean ± SEM. n=3 (ANOVA** p<0.05)

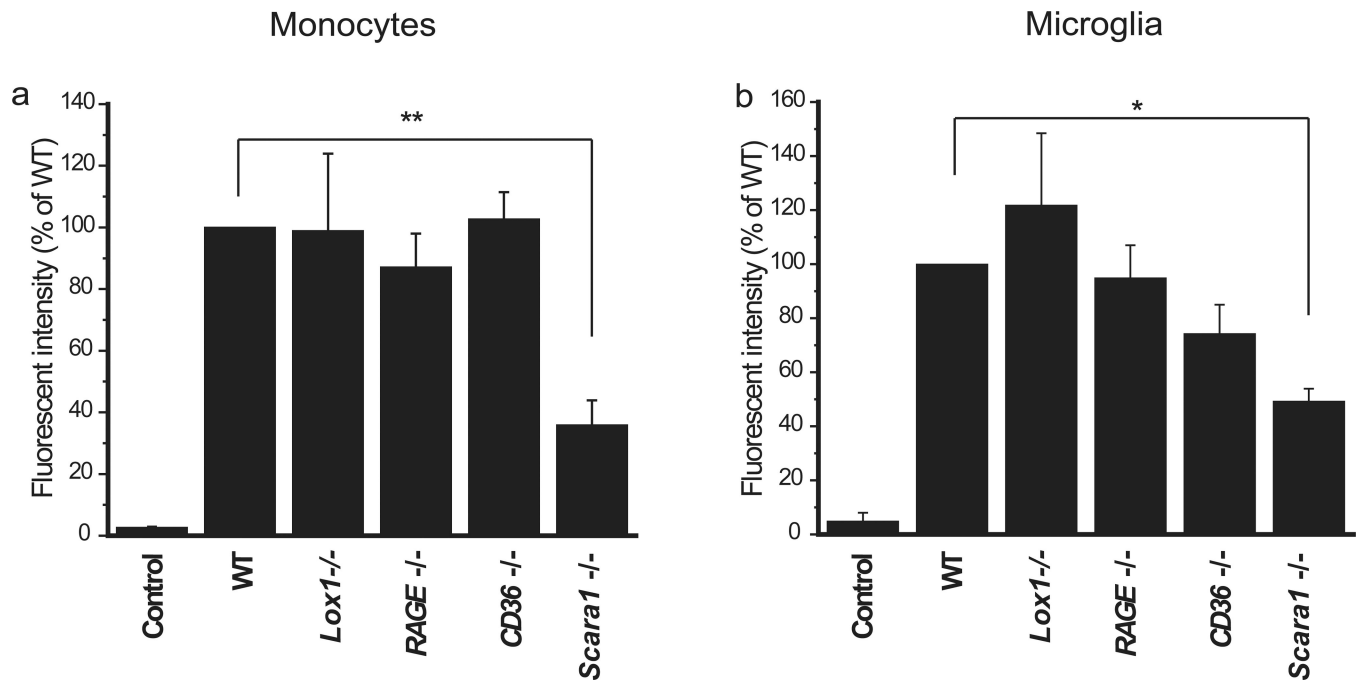


Figure 3. *Scara1* is a major monocyte and microglial receptor for sA β

Targeted deletion of *Scara1*, but not *CD36*, *LOX-1*, or *RAGE*, significantly reduces sA β uptake by CD11b⁺ monocytes (a) and microglia (b). Monocytes and microglia isolated from C57BL6 mice or mice with targeted deletion of the indicated gene were incubated with 1 μ M Hilyte fluor 488-labeled sA β 1–42 for 2 hours, and uptake of sA β was measured by flow cytometry. Data points represent the mean of triplicate determinations \pm SEM, n=4. (ANOVA, * p<0.05, ** p<0.03)

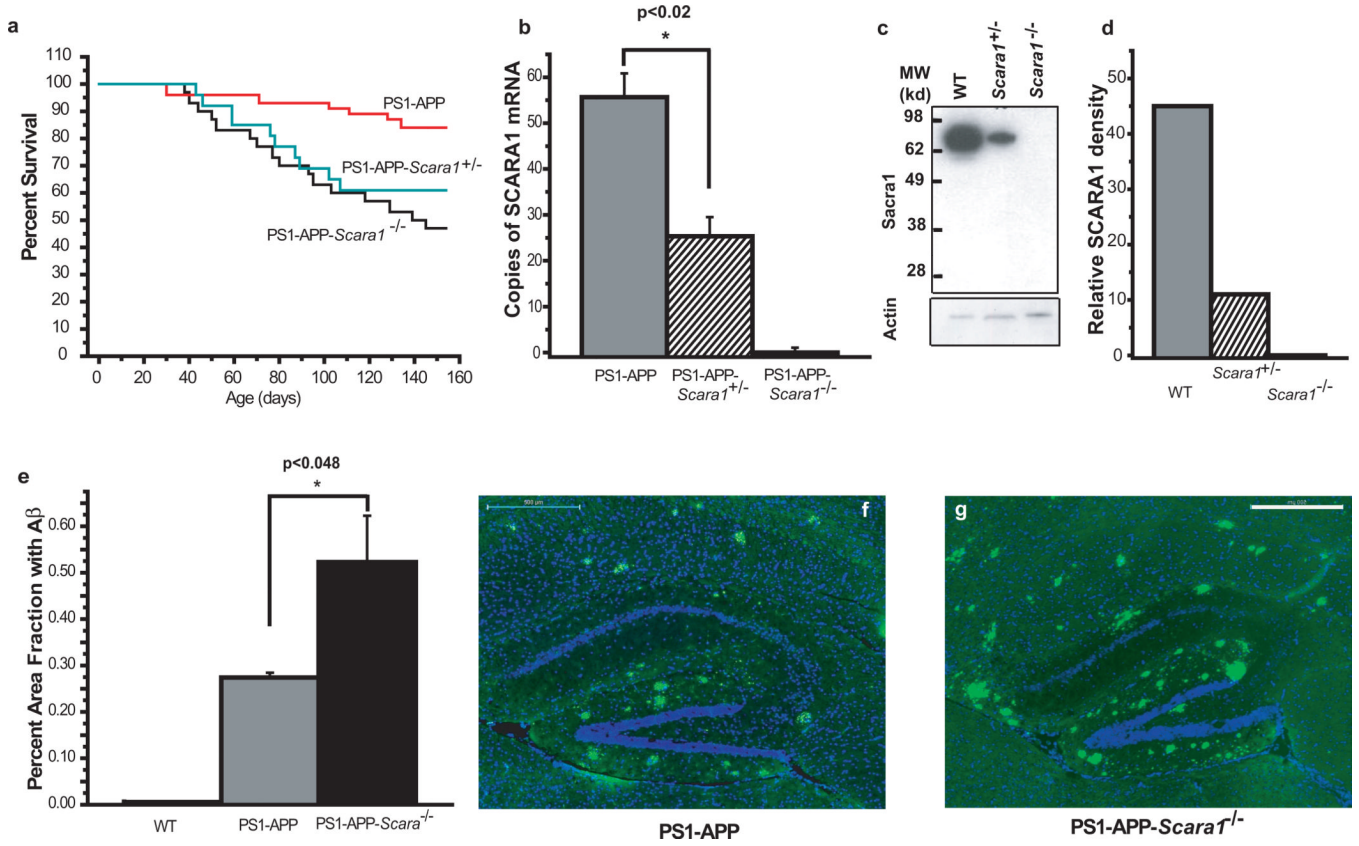


Figure 4. *Scara1* deficiency is associated with increased mortality and higher Aβ deposition in PS1-APP mice

(a) Survival curves for PS1-APP (n=30), PS1-APP-*Scara1*^{+/-} (n=25) and PS1-APP-*Scara1*^{-/-} (n=24) mice. (b) Level of *Scara1* mRNA in PS1-APP-*Scara1*^{+/-} mice is 45% that of PS1-APP mice. (c) Reduced gene dosage in *Scara1*^{+/-} mice is associated with a 76% reduction in *Scara1* protein levels as shown in this representative Western blot (c) and quantified by densitometry (d), representative blot and quantification were repeated 3 different times with similar results. (e-g) *Scara1* deficiency significantly increases Aβ deposition in 8 month-old PS1-APP mice. Increased number of visible Aβ deposits in PS1-APP-*Scara1*^{-/-} brains (g) compared to PS1-APP brains (f). Scale bars = 500μm. Data points represent the average of 5 independent determinations per mouse, ± SEM, n=4–6 mice per group. (ANOVA, *p<0.02, **p<0.048)

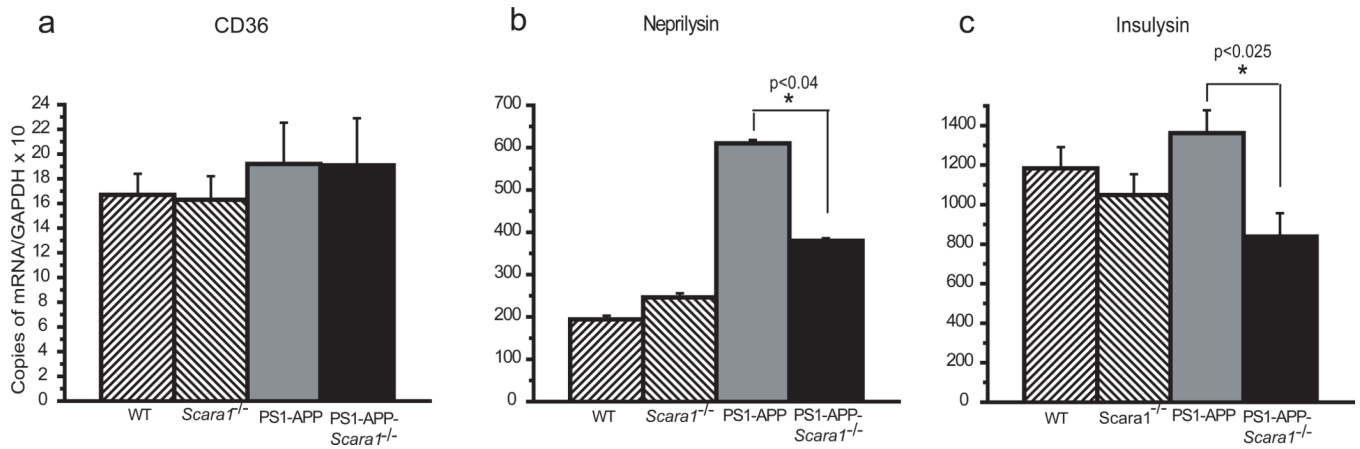


Figure 5. Effect of *Scara1* deficiency on CD36 and A β degrading enzymes
 WT and *Scara1*^{-/-} mice express comparable mRNA levels of CD36 (a), and the A β degrading enzymes neprilysin (b) and insulysin (c) in their brains. In contrast, PS1-APP-*Scara1*^{-/-} mice express similar mRNA levels of CD36 as compared to PS1-APP mice (a), but significantly lower levels of neprilysin (b) and insulysin (c). Each bar is the average of 3 triplicate determinations per mouse from 3–5 different mice per genotype \pm SEM. (ANOVA *p<0.04, **p<0.025)

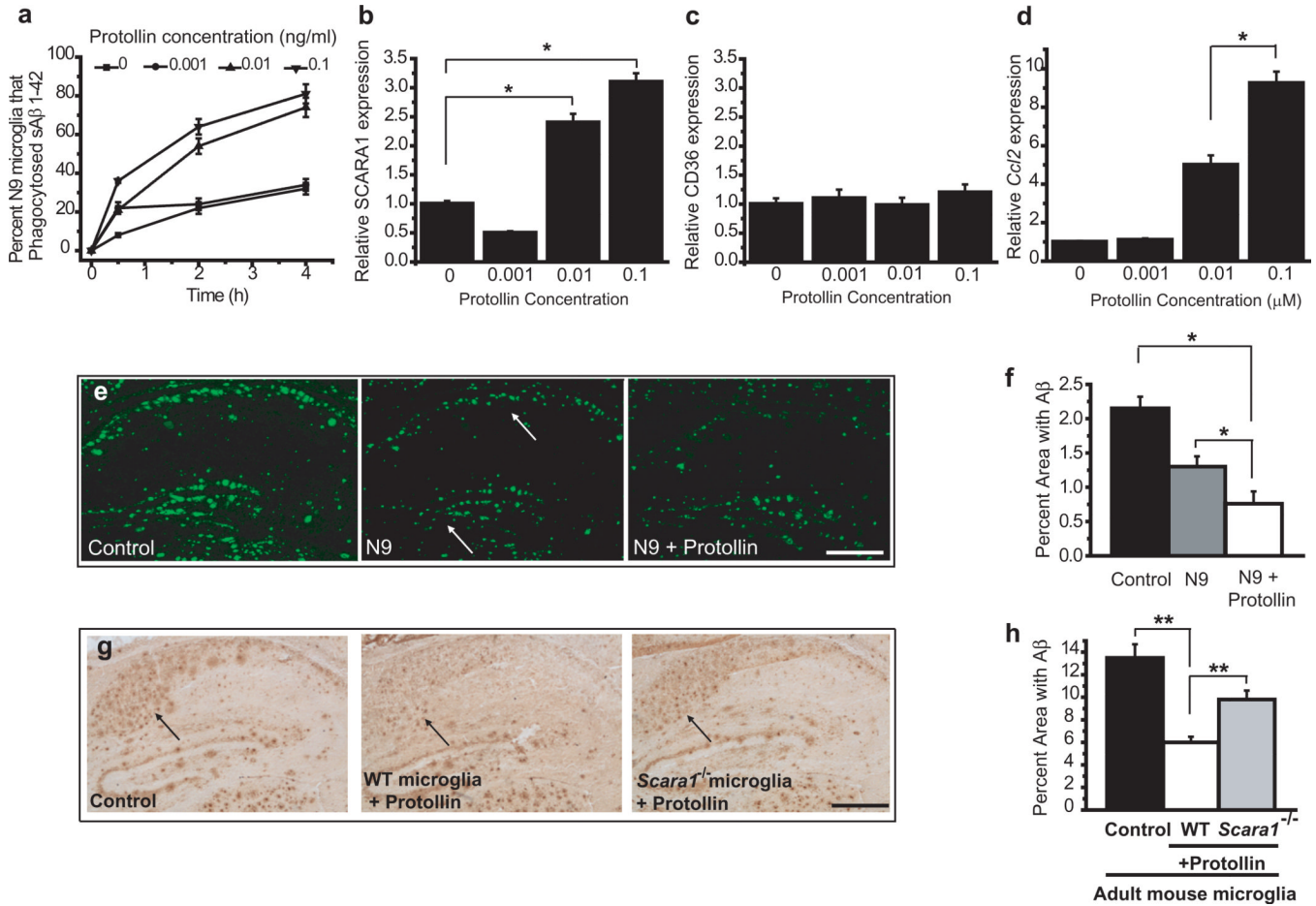


Figure 6. Upregulation of *Scar1* increases sAβ uptake *in vitro* and *in situ* in a *Scar1*-dependent mechanism

(a) Protollin, a proteasome-based adjuvant comprised of purified outer membrane proteins of *Neisseria meningitides* and lipopolysaccharide that is well tolerated in humans, upregulates sAβ uptake in N9 microglia. Cells were incubated for 18 hours in presence of different concentrations of Protollin, and incubated with 0.5 μg/ml sAβ1–42, Hilyte-fluor 488 labeled, for 30 min, 2h and 4h incubation. Cell associated sAβ was measured by flow cytometry. (b, c) Protollin upregulates *Scar1* but not CD36 expression at the transcriptional level as measured by qPCR. (d) Protollin upregulates expression of *Ccl2* in a dose-dependent manner. N9 microglia were incubated with the indicated concentration of Protollin for 24 hours, and expression of *Scar1*, *CD36* or *Ccl2* was quantified by qPCR. (e, f) N9 microglia cells are plated on brain sections from a mouse model of AD for 24h ±Protollin. The percent of the surface area of the brain covered by Aβ was measured by staining with anti-Aβ antibodies. (g, h) Reduction of amyloid load in the hippocampus following 24h incubation with microglia is *Scar1* dependent. Adult microglia isolated from WT and *Scar1*^{-/-} mice were added to brain sections from a mouse model of AD and incubated for 24h ±Protollin. The percent of the surface area of the brain covered by Aβ was measured by staining with anti-Aβ antibodies. Scale bars=500μm. All data points represent the average of 4 independent determinations ± SEM. (ANOVA* p<0.05, ** p<0.03)